Measurements of Elastic Constants in Thin Films of Colossal Magnetoresistance Material

Jin H. So, J. R. Gladden, Y. F. Hu, J. D. Maynard, and Qi Li

Department of Physics, The Pennsylvania State University, University Park, Pennsylvania 16802

(Received 15 August 2002; published 24 January 2003)

Measurements of elastic constants of strained 200 and 400 nm thin films, as well as unstrained samples, of the colossal magnetoresistance (CMR) material $La_{0.67}Ca_{0.33}MnO_3$ are presented. Since the peak resistance temperature of a strained CMR film decreases as the film thickness decreases, it is of interest to see if features in the elastic constants, reflecting structural or magnetic changes, follow the peak resistance temperature. It is observed that features in the elastic constants appear not only at the peak resistance temperatures of the CMR samples, but also at a temperature about 17 K higher. A new technique, thin-film resonant ultrasound spectroscopy, was used to make the measurements.

DOI: 10.1103/PhysRevLett.90.036103 PACS numbers: 68.60.Bs, 43.35.+d, 75.47.Gk, 75.70.Ak

The phenomenon of colossal magnetoresistance (CMR), where the electrical resistance of a material is a rapidly varying function of an applied magnetic field, is currently of considerable interest [1–5]. This effect is also of practical importance, with applications in magnetic sensors, etc. [6]. Many applications require that the material be in the form of a thin film on a substrate, and the strain which occurs during the deposition of the film alters the behavior of the material [7–9]. Experimental observations, including the effects of strain, as well as theoretical considerations indicate that there is a correlation between the CMR effect and changes in the structure of the material [10–13]. Structural changes, as well as changes in magnetic configuration, are readily probed with measurements of elastic properties, and this has been employed successfully for bulk CMR materials [14–16]. In this Letter we report the first measurements of elastic constants, together with resistivity, of both unstrained and strained (as-deposited) CMR material in the form of thin films on a substrate. Briefly, the results show that changes in the elastic constants occur at the temperature of peak resistance, which decreases as the film thickness decreases. Furthermore, changes in the elastic constants were also observed at temperatures about 17 K higher than the peak resistance temperature, which is a new result for the CMR material studied.

The CMR material used in the measurements was a doped perovskite manganite, $La_{0.67}Ca_{0.33}MnO_3$ (LCMO). Thin films were epitaxially grown on the 100 surface of $SrTiO_3$ substrates by pulsed-laser deposition. An excimer laser with a wavelength of 248 nm, an energy density of ~ 2 J/cm^2, and a repetition rate of 5 Hz was used. The growth rate was around 0.04 nm/pulse, and the thickness of the film was determined by the nominal value. The substrate temperature was around 780 °C and the oxygen pressure was about 500 mTorr during deposition. The films were cooled down in about 400 Torr of oxygen at the rate of 20 C/min after deposition. X-ray diffraction measurements indicated that all the films were epitaxially grown with the *c* axis normal to the film plane. The as-deposited films are partially strained [8]. For comparison with the measurements on the as-deposited strained films, unstrained films were obtained by annealing the films in a quartz tube at 900 °C with a flow of 50 standard cm^3/min pure O_2 for 24 h and cooled at the rate of 10 °C/min to room temperature. Previous experiments [17,18] have shown that after such annealing, films appear to have the properties of unstrained bulk CMR material. The microscopic nature of both as-deposited and annealed films has been well characterized [9].

The electrical resistance of the samples was measured with a standard four-terminal method with temperature dependence. The elastic properties of the CMR films were measured with small-sample resonant ultrasound spectroscopy (RUS). Prior to this research, RUS had been used to measure only bulk samples. The RUS method for bulk samples involves the measurement of the dimensions of a sample and a number of its natural frequencies of vibration, and the analysis of this information to determine all of the elastic constants (as well as damping coefficients) of the material. Small-sample RUS has been developed for the measurement of samples with dimensions of only a few hundred microns (and masses of less than 100 micrograms), and for such samples a thin film may constitute a measurable fraction ($\sim$ 1 part in 1000) of the entire sample. In this case, knowledge of the sample dimensions, the film thickness, the elastic constants of the substrate, and a number of measured natural frequencies is sufficient to determine all of the elastic constants of the film. A requirement of the RUS technique for small samples is that the transducers involved in the measurement be quite small themselves.

The apparatus for making RUS measurements on very small samples is illustrated in Fig. 1 [19]. In the illustration a rectangular parallelepiped sample is supported by transducers at diametrically opposite corners. Corners are used for contact because they provide elastically weak coupling to the transducers, minimizing loading, and because the corners are always elastically active (i.e., they are never nodes), and thus can be used to couple to all of

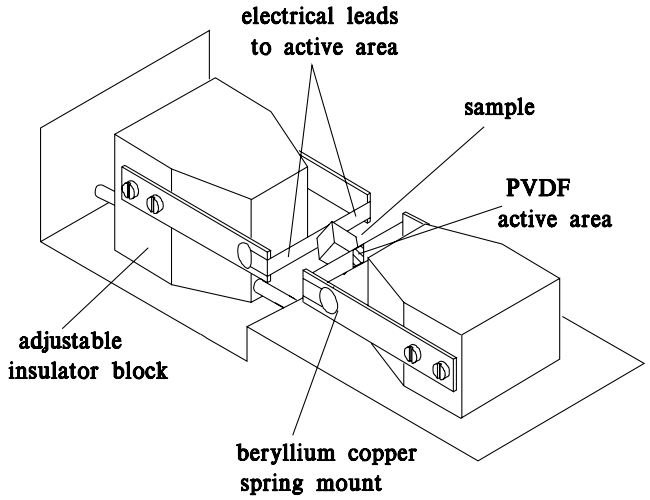

FIG. 1. Example of a RUS apparatus containing a rectangular parallelepiped sample. Two thin piezoelectric film (PVDF) transducers lightly contact the sample at its corners. One transducer excites the vibration of the sample, and the other monitors the sample response and detects resonance frequencies. Samples may be as small as a few hundred microns.

the normal modes of vibration. The two transducers in this apparatus are 9 μm thick polyvinylidene fluoride (PVDF) piezoelectric film [19], cut into strips of width $\sim$0.5 mm. The strips are partly metallized on each side, so that conducting portions overlap for $\sim$0.5 mm in the central part of the strip, forming a capacitor sandwiching the piezoelectric film. Electrical contact is made, through the metallization on the film, to metal spring mounts, which maintain a small tension in the strips. One adjustable transducer block is brought toward the other until the sample is just supported by its corners at the centers of the strips; no bonding or ultrasonic coupling agent is required. As in the general RUS measurement, one transducer drives the sample, and the other monitors the sample resonances. Because the piezoelectric film is so thin and lossy, its resonances (at relatively high frequencies) do not interfere with the sample resonances.

For the RUS measurement, small samples were cut from wafers of $SrTiO_3$, with the LCMO already deposited, and carefully polished (on sides other than the one with the film) into rectangular parallelepipeds with dimensions of approximately $1.0 \times 0.9 \times 0.3$ mm, with the film on one of the larger faces. The samples, mounted in the RUS apparatus, were sealed in a cell with helium exchange gas and cooled in a cryostat, with the temperature regulated to within a few millikelvin. At each temperature, six to eight resonances, selected for having the greatest dependence on the C_{11} and C_{44} elastic constants for the film, were measured. After 200 and 400 nm as-deposited films were measured, the 400 nm sample was annealed and remeasured. Finally, the LCMO films were chemically removed, and the resonance frequencies for the bare $SrTiO_3$ substrates were measured. The elastic properties of the various films were determined from the shifts in the resonance frequencies of the samples with and without the films.

The crystal structure of LCMO may be considered as basically orthorhombic, but with some (e.g., Jahn-Teller) distortions to lower symmetry. In determining elastic constants with RUS, the measurement of a sufficient number of resonance frequencies allows one to find all of the elastic constants for orthorhombic or even lower symmetry. However, in our data analysis, we determine just two effective elastic constants, referred to as C_{11} and C_{44}. If the material were cubic and effectively isotropic, then these would reflect all of the elastic properties, with C_{11} and C_{44} being the longitudinal and shear moduli, respectively. To a good approximation, our C_{11} and C_{44} are close to longitudinal and shear moduli for films of LCMO on $SrTiO_3$, for several reasons: (i) in the basic orthorhombic structure, the deviations from cubic are small, about 1%–2%, (ii) in an LCMO film of thickness greater than 50 nm, the orthogonal orientations occur with equal frequency in domains of size $\sim$100 nm, (iii) the RUS measurement averages over acoustic wavelengths of $\sim$100 μm, and (iv) other observations on LCMO indicate almost isotropic characteristics [9]. Similar assumptions were made in the analysis of elastic

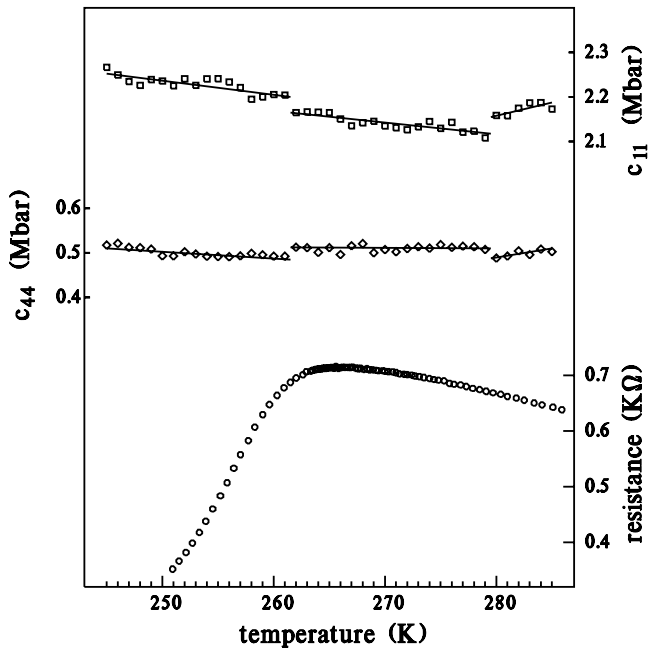

FIG. 2. Experimentally measured elastic constants c_{11} and c_{44} and the electrical resistance of unstrained LCMO as functions of temperature. The squares are c_{11}, the diamonds are c_{44} (with the upper scales), and the circles are electrical resistance (with the lower scale on the right). Features in the elastic constants are evident not only at 262 K (near the temperature of maximum resistance), but also about 17 K higher. The lines are piecewise least-square fits.

data for (La, Sr)MnO_3 [15]. In any case, our main interest is in the temperature dependence of the elastic properties, and this could be seen with a presentation of the raw resonance frequency data. The analysis producing the effective C_{11} and C_{44} may be considered as an educated reduction (simplification) of the raw frequency data.

The electrical resistance and elastic properties for the annealed LCMO are shown in Fig. 2. Experimental results [17,18] indicate that the properties of annealed films of thickness greater than 50 nm are the same as for bulk material, so the results discussed here may be compared with those of bulk $La_{0.67}Ca_{0.33}MnO_3$. Indeed, the temperature of the resistance peak and the features in the elastic constants (jumps of a few percent) at 262 K agree well with the temperature of ~260 K where one typically observes the bulk resistance peak [16,20], magnetic effects [13], and changes in ultrasound speed and attenuation [16]. However, the data in Fig. 2 also show a jump of a few percent in the elastic constants at 279 K, about 17 K higher than the other jump. It is interesting to note that a higher temperature feature may be seen in neutron scattering measurements on single crystals [13] and powder samples [21], some volume change measurements [10], and ultrasound attenuation measurements [16], but these features were not discussed in the published papers. In our measurements, temperature was swept in both directions, and little or no hysteresis was observed (less than a few Kelvin).

Deviating from bulk material, strained films are known to have lower resistance peak temperatures (decreasing from the bulk value as film thickness decreases), and it would be of interest to see if two elastic constant features are present in strained films, and if they are at lower temperatures, tracking the peak resistance temperature.

The elastic constants and electrical resistance of the strained 400 and 200 nm films are presented in Figs. 3 and 4. Two characteristics of the elastic behavior common to the strained films are observed. First, there are a number of features in the elastic properties (primarily in C_{11}) as the temperature is swept monotonically which do not repeat if the sample is thermally cycled. These changes may be due to thermal-stress induced, irreversible changes in the fine-scale structure of the as-deposited films [15]. Second, there are features which do occur reproducibly at two temperatures, and these are indicated by jumps and/or, in nearly all cases, by changes in slope. For the 400 nm sample results shown in Fig. 3, such features occur at 256 and 273 K, with the peak in the resistance at ~256 K. For the 200 nm sample results shown in Fig. 4, the changes are evident at 251 and

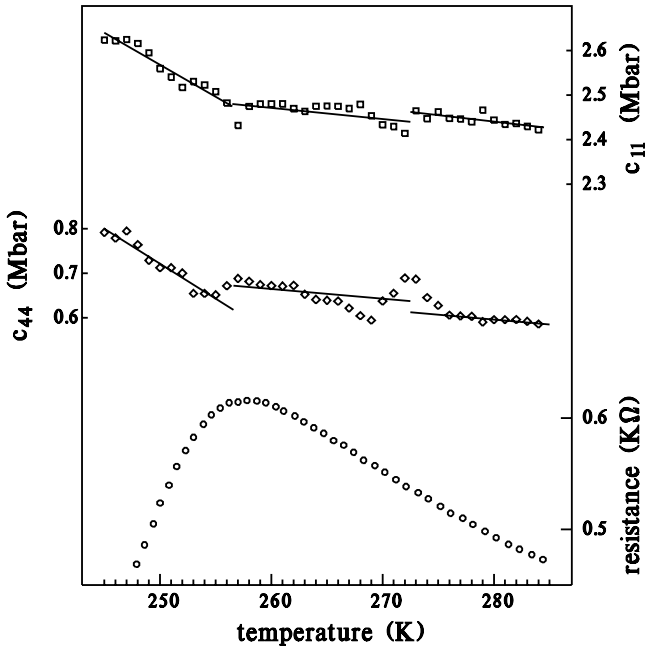

FIG. 3. Experimentally measured elastic constants c_{11} and c_{44} and the electrical resistance of a strained 400 nm LCMO thin film as functions of temperature. The squares are c_{11}, the diamonds are c_{44} (with the upper scales), and the circles are electrical resistance (with the lower scale on the right). A transition in the elastic constants at 273 K as well as a transition near the peak resistance temperature (at 256 K) are evident. The lines are piecewise least-square fits.

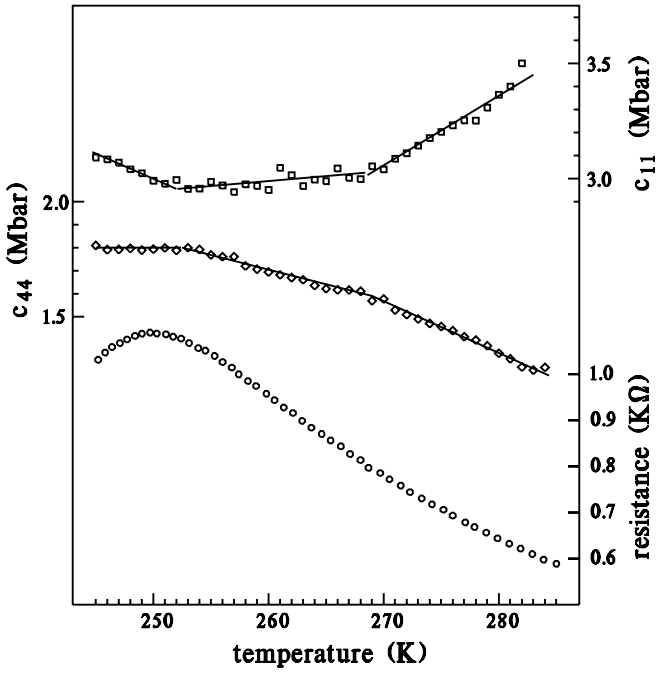

FIG. 4. Experimentally measured elastic constants c_{11} and c_{44} and the electrical resistance of a strained 200 nm LCMO thin film as functions of temperature. The squares are c_{11}, the diamonds are c_{44} (with the upper scales), and the circles are electrical resistance (with the lower scale on the right). A transition in the elastic constants at 269 K as well as a transition near the peak resistance temperature (at 252 K) are evident. The lines are piecewise least-square fits.

268 K, when the peak in the resistance is at ~251 K. Thus the two features in the elastic constants do exist for strained films, and more interestingly, they track the changes in the peak resistance temperature.

Some discussion relevant to the nature of the two features in the elastic constants would be appropriate. Because of the interplay among the effects of charge localization, lattice distortion, and magnetic ordering, there are a number of possibilities. One of the features probably coincides with the para-to-ferro magnetic transition. As for the second feature, the phase diagram for $La_{1-x}Ca_xMnO_3$ is rich in candidate features, many of which have received thorough investigation [22]. Of particular interest, in regard to elastic constants, is the presence of a structural transition which is separate from the magnetic transitions except when x approaches 0.20 [22]. A related material, (La, Sr)MnO_3, has a similar structural transition, and this transition shows readily observed hysteresis [11,15]. However, for $La_{1-x}Ca_xMnO_3$ with $x > 0.2$ there seems to be no further mention of a structural transition in the literature. For speculations about either of the elastic constant features, we summarize our observations as follows: (i) There was no significant hysteresis. (ii) The two features appeared in both the as-deposited and annealed samples. (iii) One feature always appeared near the resistance peak and the other appeared about 17 K higher.

This research was supported by the National Science Foundation Grants No. DMR9801844 and No. DMR9876266 and by the Office of Naval Research.

[1] R. M. von Helmholt, J. Wecker, B. Holzapfel, L. Schultz, and K. Samwer, Phys. Rev. Lett. **71**, 2331 (1993).
[2] S. Jin, T. H. Tiefel, M. McCormack, R. A. Fastnacht, R. Ramesh, and L. H. Chen, Science **264**, 413 (1994).
[3] A. P. Ramirez, J. Phys. Condens. Matter **9**, 8171 (1997).
[4] V. M. Loktev and Yu. G. Pogorelov, Low Temp. Phys. **26**, 171 (2000).
[5] A. J. Millis, Nature (London) **392**, 147 (1998).
[6] J. Z. Sun, W. J. Gallagher, P. R. Duncombe, L. Krusin-Elbaum, R. A. Altman, A. Gupta, Y. Lu, G. Q. Gong, and G. Xiao, Appl. Phys. Lett. **69**, 3266 (1996).
[7] H. S. Wang and Q. Li, Appl. Phys. Lett. **73**, 2360 (1998).
[8] H. S. Wang, E. Wertz, Y. F. Hu, Qi Li, and D. G. Schlom, J. Appl. Phys. **87**, 7409 (2000).
[9] C. J. Lu, Z. L. Wang, C. Kwon, and X. Jia, J. Appl. Phys. **88**, 4032 (2000).
[10] J. M. De Teresa, M. R. Ibarra, J. Blasco, J. Garcia, C. Marquina, P. A. Algarabel, Z. Arnold, K. Kamenev, C. Ritter, and R. von Helmolt, Phys. Rev. B **54**, 1187 (1996).
[11] A. Asamitsu, Y. Moritomo, R. Kumai, Y. Tomioka, and Y. Tokura, Phys. Rev. B **54**, 1716 (1996).
[12] P. Dai, J. Zhang, H. A. Mook, S-H. Liou, P. A. Dowben, and E. W. Plummer, Phys. Rev. B **54**, R3694 (1996).
[13] Q. Huang, A. Santoro, J. W. Lynn, R. W. Erwin, J. A. Borchers, J. L. Peng, K. Ghosh, and R. L. Greene, Phys. Rev. B **58**, 2684 (1998).
[14] A. P. Ramirez, P. Schiffer, S-W. Cheong, C. H. Chen, W. Bao, T. T. M. Palstra, P. L. Gammel, D. J. Bishop, and B. Zegarski, Phys. Rev. Lett. **76**, 3188 (1996).
[15] T. W. Darling, A. Migliori, E. G. Moshopoulou, S. A. Trugman, J. J. Nuemeier, J. L. Sarro, A. R. Bishop, and J. D. Thompson, Phys. Rev. B **57**, 5093 (1998).
[16] C. Zhu, R. Zheng, J. Su, and J. He, Appl. Phys. Lett. **74**, 3504 (1999).
[17] M. F. Hundley, M. Hawley, R. H. Hefner, Q. X. Jia, J. J. Neumeier, J. Tesmer, J. D. Thompson, and X. D. Wu, Appl. Phys. Lett. **67**, 860 (1995).
[18] S. E. Lofland, S. M. Bhagat, H. L. Ju, G. C. Xiong, T. Venkatesan, and R. L. Greene, Phys. Rev. B **52**, 15 058 (1995).
[19] Julian D. Maynard, J. Acoust. Soc. Am. **91**, 1754 (1992).
[20] P. Schiffer, A. P. Ramirez, W. Bao, and S-W. Cheong, Phys. Rev. Lett. **75**, 3336 (1995).
[21] C. P. Adams, J. W. Lynn, Y. M. Mukovskii, A. A. Arsenov, and D. A. Shulyatev, Phys. Rev. Lett. **85**, 3954 (2000).
[22] G. Biotteau, M. Hennion, F. Moussa, J. Rodríguez-Caravajal, L. Pinsard, A. Revcolevschi, Y. M. Mukovskii, and D. Shulyatev, Phys. Rev. B **64**, 104421 (2001).